molecular pharmaceutics

articles

Disposition of Formononetin via Enteric Recycling: Metabolism and Excretion in Mouse Intestinal Perfusion and Caco-2 Cell Models

Eun Ju Jeong,[†] Xiaobin Jia,[‡] and Ming Hu*

Department of Pharmacological and Pharmaceutical Sciences, College of Pharmacy, University of Houston, Houston, Texas 77030

Received December 22, 2004

Abstract: The purpose of this study was to determine the absorption and metabolism of formononetin using the mouse intestinal perfusion model, mouse intestinal homogenate, and the Caco-2 cell culture model. In the perfusion model where upper and lower small intestine were perfused simultaneously, absorption of formononetin was rapid and dimensionless effective permeabilities of formononetin (2.53−2.90) were similar to those for rats. Moreover, the amounts of sulfates excreted in mouse intestine (8−11 nmol/30 min/10 cm) were significantly higher than those for rats whereas the amounts of glucuronides excreted (7−10 nmol/30 min/10 cm) were comparable. Small amounts of formononetin glucuronide but not sulfate were found in mouse bile, but the total amounts were 120 times less than those for rats. Multidrug-resistance-related protein (MRP) inhibitors (leukotriene C_4 plus MK-571, $C_{26}H_{26}ClN_2O_3S_2$) significantly decreased the excretion of glucuronide and sulfate in mouse intestine (52−74% for glucuronide, 13−26% for sulfate) and in Caco-2 cells (92% for glucuronide, 37% for sulfate). They also inhibited formation of conjugates in intestinal homogenate (∼60% for glucuronide, ∼30% for sulfate) and Caco-2 cell lysate (∼92% for glucuronide, ∼37% for sulfate). Organic anion transporter (OAT) inhibitors (estrone sulfate plus dihydroepiandrosterone sulfate) did not significantly change the excretion of formononetin conjugates in either model, even though they significantly decreased the formation of both. In conclusion, our study showed that formononetin has similar absorption in rat and mouse intestine, but metabolism was species-dependent. The mouse perfusion model may have an advantage over the rat intestinal perfusion model for flavonoid disposition studies in that both sulfates and glucuronides are excreted, as shown in humans.

Keywords: Conjugates; coupling; excretion; mouse intestine; perfusion; formononetin

Introduction

Flavonoids belong to an important class of phytochemicals that are gathering increasing interest in clinical nutrition and disease prevention.[1−4] Flavonoids including isoflavones have health benefits in aging-related and hormone-dependent disorders, including but not limited to cancer, peri- and postmenopausal symptoms, cardiovascular disease, and osteoporosis.[1,2,5−8]

Flavonoids have poor bioavailabilities (generally less than 5%), which can vary considerably among individuals.[6,9−12] The poor bioavailability of flavonoids is attributed to the

* To whom correspondence should be addressed. Mailing address: Department of Pharmacological and Pharmaceutical Sciences, 1441 Moursund St., College of Pharmacy, University of Houston, Houston, TX 77030. Tel: 713-795-8320. Fax: 713-795-8305. E-mail: mhu@uh.edu.

[†] Present address: Korea Institute of Toxicology, Korea Research Institute of Chemical Technology, Daejeon, Republic of Korea, 305-600.

[‡] Present address: Jiangsu Provincial Academy of Traditional Chinese Medicine, Nanjing, China, 210028.

(1) Tham, D. M.; Gardner, C. D.; Haskell, W. L. Clinical review 97: potential health benefits of dietary phytoestrogens: a review of the clinical, epidemiological, and mechanistic evidence. *J. Clin. Endocrinol. Metab.* **1998**, *83*, 2223−2235.

(2) Setchell, K. D. R.; Cassidy, A. Dietary isoflavones: biological effects and relevance to human health. *J. Nutr.* **1999**, *129*, 758S−767S.

10.1021/mp0498852 CCC: $30.25 © 2005 American Chemical Society
Published on Web 05/27/2005

extensive metabolism, since their absorption in the intestine is very rapid.[13−18] It was long believed that the main site of flavonoid metabolism is the liver,[5] as evidenced by large amounts of conjugates in bile and/or feces.[19,20] Recently, several groups of investigators including ourselves have shown that the intestine metabolized flavonoids via phase II pathways and excreted their conjugates.[13−18,21] Major metabolites of flavonoids in humans are glucuronides and sulfates.[22]

Poor bioavailabilities of flavonoids may prevent their development into viable chemopreventive agents, especially if the aglycons were proven to be the active ingredients. Therefore, understanding the mechanisms responsible for their poor bioavailabilities is essential to improve their chance of becoming successful chemopreventive agents. Previously, we have hypothesized that participation in dual recycling via enteric and enterohepatic processes is the reason why flavonoids have poor bioavailabilities. We have shown recently that the recycling is enabled by the coupling of efflux transporters and conjugating enzymes (or "enzyme-transporter coupling") in gut and liver.[17,23] The recycling processes, though limiting the bioavailability of flavonoids, provide a prolonged period of systemic exposure to flavonoid conjugates, which maintain significant antioxidant properties.

The development of an additional model that can be used to better study the mechanisms involved in formation and excretion of both glucuronides and sulfates is required to understand the intricate biodistribution process of flavonoids in vivo. This is because the perfused rat intestinal model used in the majority of the disposition studies does not excrete significant amounts of flavonoid sulfates (especially at lower concentrations). Both glucuronidated and sulfated conjugates were reported to present in human plasma and urine.[23−26] Some glucuronides, such as daidzein and genistein glucuronides, have weak estrogenic properties and enhance human natural killer cell activities in vitro.[27] Genistein-7-sulfate and biochanin A sulfate were detected in human breast cancer cell lines after incubation with radiolabeled genistein and biochanin A, but the sulfates were not active forms in these cancer cell lines.[28]

(3) Messina, M. J. Legumes and soybeans: overview of their nutritional profiles and health effects. *Am. J. Clin. Nutr.* **1999**, *70*, 439S−450S.

(4) Jacobsen, B. K.; Knutsen, S. F.; Fraser, G. E. Does high soy milk intake reduce prostate cancer incidence? The Adventist Health Study (United States). *Cancer, Causes Control* **1998**, *9*, 553−557.

(5) Kurzer, M.; Xu, X. Dietary phytoestrogens. *Annu. Rev. Nutr.* **1997**, *17*, 353−381.

(6) Birt, D. F.; Hendrich, S.; Wang, W. Dietary agents in cancer prevention: flavonoids and isoflavonoids. *Pharmacol. Ther.* **2001**, *90*, 157−177.

(7) Yang, C. S.; Landau, J. M.; Huang, M. T.; Newmark, H. L. Inhibition of carcinogenesis by dietary polyphenolic compounds. *Annu. Rev. Nutr.* **2001**, *21*, 381−406.

(8) Harborne, J. B.; Williams, C. A. Advances in flavonoid research since 1992. *Phytochemistry* **2000**, *55*, 481−504.

(9) Kelly, G. E.; Joannou, G. E.; Reeder, A. Y.; Nelson, C.; Waring, M. A. The variable metabolic response to dietary isoflavones in humans. *Proc. Soc. Exp. Biol. Med.* **1995**, *208*, 40−43.

(10) Setchell, K. D. Phytoestrogens: the biochemistry, physiology, and implications for human health of soy isoflavones. *Am. J. Clin. Nutr.* **1998**, *68*, 1333S−1346S.

(11) Setchell, K. D.; Brown, N. M.; Desai, P.; Zimmer-Nechemias, L.; Brashear, W. T.; Kirschner, A. S.; Cassidy, A.; Heubi, J. E. Bioavailability of pure isoflavones in healthy humans and analysis of commercial soy isoflavone supplements. *J. Nutr.* **2001**, *131*, 1362S−1375S.

(12) Busby, M. G.; Jeffcoat, A. R.; Bloedon, L. T.; Koch, M. A.; Black, T.; Dix, K. J.; Heizer, W. D.; Thomas, B. F.; Hill, J. M.; Crowell, J. A.; Zeisel, S. H. Clinical characteristics and pharmacokinetics of purified soy isoflavones: single-dose administration to healthy men. *Am. J. Clin. Nutr.* **2002**, *75*, 126−136.

(13) Crespy, V.; Morand, C.; Manach, C.; Besson, C.; Demigne, C.; Remesy, C. Part of quercetin absorbed in the small intestine is conjugated and further secreted in the intestinal lumen. *Am. J. Physiol.* **1999**, *277*, G120−G126.

(14) Walle, U. K.; Galijatovic, A.; Walle, T. Transport of the flavonoid chrysin and its conjugated metabolites by the human intestinal cell line Caco-2. *Biochem. Pharmacol.* **1999**, *58*, 431−438.

(15) Andlauer, W.; Kolb, J.; Furst, P. Isoflavones from tofu are absorbed and metabolized in the isolated rat small intestine. *J. Nutr.* **2000**, *130*, 3021−3027.

(16) Liu, Y.; Hu, M. Absorption and metabolism of flavonoids in the caco-2 cell culture model and a perfused rat intestinal model. *Drug Metab. Dispos.* **2002**, *30*, 370−307.

(17) Chen, J.; Lin, H.; Hu, M. Metabolism of Flavonoids via Enteric Recycling: Role of Intestinal Disposition. *J. Pharmacol. Exp. Ther.* **2003**, *304*, 1228−1235.

(18) Jia, X.; Chen, J.; Lin, H.; Hu, M. Disposition of flavonoids via enteric recycling: enzyme-transporter coupling affects metabolism of biochanin A and formononetin and excretion of their phase II conjugates. *J. Pharmacol. Exp. Ther.* **2004**, *310*, 1103−1113.

(19) Xu, X.; Harris, K. S.; Wang, H. J.; Murphy, P. A.; Hendrich, S. Bioavailability of soybean isoflavones depends upon gut microflora in women. *J. Nutr.* **1995**, *125*, 2307−2315.

(20) King, R. A.; Broadbent, J. L.; Head, R. J. Absorption and excretion of the soy isoflavone genistein in rats. *J. Nutr.* **1996**, *126*, 176−182.

(21) Hu, M.; Chen, J.; Lin, H. Metabolism of Flavonoids via Enteric Recycling: Mechanistic Studies of Disposition of Apigenin in the Caco-2 Cell Culture Model. *J. Pharmacol. Exp. Ther.* **2003**, *307*, 314−321.

(22) Clarke, D. B.; Lloyd, A. S.; Botting, N. P.; Oldfield, M. F.; Needs, P. W.; Wiseman, H. Measurement of intact sulfate and glucuronide phytoestrogen conjugates in human urine using isotope dilution liquid chromatography-tandem mass spectrometry with [13C(3)]-isoflavone internal standards. *Anal. Biochem.* **2002**, *309*, 158−172.

(23) Jeong, E. J.; Liu, Y.; Lin, H.; Hu, M. Species- and Disposition Model-Dependent Metabolism of Raloxifene in Gut and Liver: Role of UGT1A10. *Drug Metab Dispos*. **2005**, Mar 15 (Internet), 10.1124/dmd.104.001883.

(24) Shelnutt, S. R.; Cimino, C. O.; Wiggins, P. A.; Badger, T. M. Urinary pharmacokinetics of the glucuronide and sulfate conjugates of genistein and daidzein. *Cancer Epidemiol., Biomarkers Prev.* **2000**, *9*, 413−419.

(25) Shelnutt, S. R.; Cimino, C. O.; Wiggins, P. A.; Ronis, M. J.; Badger, T. M. Pharmacokinetics of the glucuronide and sulfate conjugates of genistein and daidzein in men and women after consumption of a soy beverage. *Am. J. Clin. Nutr.* **2002**, *76*, 588−594.

(26) Zhang, Y.; Hendrich, S.; Murphy, P. A. Glucuronides are the main isoflavone metabolites in women. *J. Nutr.* **2003**, *133*, 399−404.

In the present study, we investigated the intestinal absorption and metabolism of formononetin using the single-pass mouse intestinal perfusion model along with the Caco-2 cell culture model. This represents one of the first reports of extending the popular rat intestinal perfusion model to mouse intestinal perfusion. The "two-site" mouse perfusion model used here was adapted from our "four-site" single-pass rat intestinal perfusion model.[29] We chose formononetin for this study because it has only one phenol group and is ideally suited to determine the relative fidelity of glucuronidation versus sulfation pathway. It is also chosen since the excretion of its glucuronidated metabolite in rat intestine is very rapid, allowing selective and accurate quantification of the conjugates.[18]

Experimental Section

Materials. Cloned Caco-2 cells, TC7, were a kind gift from Dr. Monique Rousset (Institut National de la Sante et de la Recherche Medicale U178, Villejuit, France). Formononetin was purchased from Indofine Chemicals (Somerville, NJ). β-Glucuronidase with (Catalog No. G1512) or without sulfatase (Catalog No. G7396), sulfatase without glucuronidase (Catalog No. S1629), uridine diphosphoglucuronic acid, alamethicin, D-saccharic acid 1,4-lactone monohydrate, magnesium chloride, Tris, phenylmethylsulfonyl fluoride (PMSF) and Hanks' balanced salt solution (HBSS, powder form) were purchased from Sigma-Aldrich (St. Louis, MO). All other materials (typically analytical grade or better) were used as received.

Cell Culture. The culture conditions for growing Caco-2 cells have been described previously.[16,30,31] The seeding density (100 000 cells/cm^2), growth media (Dulbecco's modified Eagle's medium supplemented with 10% fetal bovine serum), and quality control criteria were all implemented in the present study as they were described previously.[30,31] Caco-2 TC7 cells were fed every other day, and cell monolayers (4.2 cm^2 total areas) were ready for experiments from 19 to 21 days postseeding.

Transport Experiments in the Caco-2 Cell Culture Model. The protocol for performing cell culture experiments is the same as that described previously.[16,32] Briefly, the cell monolayers were washed three times with 37 °C, pH 7.4 HBSS. The transepithelial electrical resistance values were measured, and those with transepithelial electrical resistance values less than 450 Ω cm^2 were discarded. The monolayers were incubated with the buffer for 1 h, and the incubation medium was then aspirated. Afterward, 10 μM formononetin in pH 7.4 HBSS was loaded at the apical side of the Caco-2 cell monolayer, and the concentrations of formononetin and its metabolites at both sides were measured by HPLC. Inhibitors, when used, were loaded at the beginning of the experiment to both sides of the monolayer. Six samples (650 μL each) were taken at different times (0, 30, 60, 90, and 120 min and 7 h after incubation) from both donor and receiver sides (total volume of each chamber is 2.5 mL), and the same volume of donor solution (containing formononetin or formononetin plus inhibitors) or receiver medium (pH 7.4 HBSS or pH 7.4 HBSS plus inhibitors) was replaced after each sampling. Forty-five microliters of internal standard solution (100 μM testosterone in 94% acetonitrile/6% glacial acetic acid) was immediately added to 200 μL of samples to stabilize them until analysis. The mixture was centrifuged at 13 000 rpm for 8 min, and the supernatant was analyzed by HPLC.

Animals. Male CB6F1 mice (9−11 weeks old) weighing between 26 and 34 g were obtained from Jackson Laboratory (Bar Harbor, ME). The mice were fed with Teklad F6 rodent diet (W) from Harlan Laboratories (Madison, WI) for at least 1 week prior to actual experiments. The mice were fasted overnight. No flavonoids were found in pH 7.4 HBSS buffer that had been perfused through a segment of intestine, indicating minimal presence of dietary flavonoids in the intestine at the time of the experiment.

Animal Surgery. The intestinal surgical procedures were modified from our previous publications,[29,33,34] in that we perfused two segments of small intestine simultaneously (a "two-site model") because of the shorter length of mouse small intestine (total ~25 cm) than rat small intestine (total ~80 cm). The bile sample was obtained from the gall bladder at the end of the experiment. To keep the temperature of the perfusate constant, the inlet cannula was insulated and kept warm by a 37 °C circulating water bath.

Transport and Metabolism Experiments in the Perfused Mouse Intestinal Model. Single-pass intestinal per-

(27) Zhang, Y.; Song, T. T.; Cunnick, J. E.; Murphy, P. A.; Hendrich, S. Daidzein and genistein glucuronides in vitro are weakly estrogenic and activate human natural killer cells at nutritionally relevant concentrations. *J. Nutr.* **1999**, *129*, 399−405.

(28) Peterson, T. G.; Ji, G. P.; Kirk, M.; Coward, L.; Falany, C. N.; Barnes, S. Metabolism of the isoflavones genistein and biochanin A in human breast cancer cell lines. *Am. J. Clin. Nutr.* **1998**, *68*, 1505S−1511S.

(29) Jeong, E. J.; Liu, Y.; Lin, H.; Hu, M. In situ single-pass perfused rat intestinal model for absorption and metabolism, Optimization in drug discovery—in vitro methods. In *Methods in Pharmacology and toxicology*; Yan, Z., Caldwell, G. W., Eds.; Humana Press: Totowa, NJ, 2004; pp 65−76.

(30) Hu, M.; Chen, J.; Tran, D.; Zhu, Y.; Leonardo, G. The Caco-2 cell monolayers as an intestinal metabolism model: metabolism of dipeptide Phe-Pro. *J. Drug Targeting* **1994**, *2*, 79−89.

(31) Hu, M.; Chen, J.; Zhu, Y.; Dantzig, A. H.; Stratford, R. E., Jr.; Kuhfeld, M. T. Mechanism and kinetics of transcellular transport of a new β-lactam antibiotic loracarbef across an human intestinal epithelial model system (Caco-2). *Pharm. Res.* **1994**, *11*, 1405−1413.

(32) Jeong, E. J.; Lin, H.; Hu, M. Disposition mechanisms of raloxifene in the human intestinal Caco-2 model. *J. Pharmacol. Exp. Ther.* **2004**, *310*, 376−385.

(33) Hu, M.; Roland, K.; Ge, L.; Chen, J.; Tyle, P.; Roy, S. Determination of absorption characteristics of AG337, a novel thymidylate synthase inhibitor, using a perfused rat intestinal model. *J. Pharm. Sci.* **1998**, *87*, 886−890.

(34) Hu, M.; Sinko, P. J.; DeMeere, A. L. J.; Johnson, D. A.; Amidon, G. L. Membrane permeability parameters for some amino acids and β-lactam antibiotics: application of the boundary layer approach. *J. Theor. Biol.* **1988**, *131*, 107−114.

fusion was performed in mouse by adapting the method used in rats[17,29] with some modifications. Two segments of small intestine (first and last 10 cm of the small intestine) were perfused simultaneously at a flow rate of 0.191 mL/min with a perfusate containing the 10 μM formononetin in pH 7.4 HBSS supplemented with 20 mM sodium chloride using an infusion pump (model PHD2000; Harvard Apparatus, Cambridge, MA). Inhibitors, when used, were added to the perfusate containing 10 μM formononetin before the experiment. After a 30 min washout period with perfusate, which is usually sufficient to achieve the steady-state absorption, four samples were collected from the outlet cannula every 30 min. The bile duct was tied before the intestine, and bile was allowed to accumulate inside the gallbladder before and during the perfusion. At the end of perfusion, bile samples were collected by tying the liver side of the bile duct and then carefully removing the gallbladder with scissors. The gallbladder was weighed before and after accumulated bile was removed, and amount of bile was then determined. After perfusion, the length of the intestine was measured as described previously.[18,33,34] The outlet concentrations of formononetin and its metabolites in the perfusate were determined by HPLC. Bile samples from 4 mice were pooled, and glucuronidase plus sulfatase or glucuronidase alone was added to portions of the bile and reacted for 6 h to release formononetin for HPLC measurement.

Preparation of Mouse Intestinal Homogenate. Mouse intestinal homogenate was prepared from adult mice using a procedure adopted from our earlier works in the preparation of rat intestinal microsomes[17,23] with modification. The mice, which were fasted overnight, were anesthetized with ip injection of urethane (2.6 g/kg). Segments of two mouse small intestines were cut and separated using the following protocol: first 10 cm, upper small intestine; last 10 cm, lower small intestine. After flushing with ice cold saline containing 1 mM dithiothreitol, each segment was cut open lengthwise and washed twice with ice-cold solution A, consisting of 8 mM KH_2PO_4, 5.6 mM Na_2HPO_4, 1.5 mM KCl, 96 mM NaCl, and 0.04 mg/mL phenylmethylsulfonyl fluoride (PMSF). The intestinal strips were blot dried and scraped, and the scraped mucosal cells were put into ice-cold solution B, consisting of 8 mM KH_2PO_4, 5.6 mM Na_2HPO_4, 1.5 mM EDTA, 0.5 mM dithiothreitol, and 0.04 mg/mL PMSF. Cells were collected by centrifugation at 900*g*, 5 min, and washed twice with homogenization buffer consisting of pH 7.4 10 mM KH_2PO_4, 250 mM sucrose, 5.6 mM Na_2HPO_4, and 0.04 mg/mL PMSF. The cells were resuspended in 1−2 mL of homogenization buffer and homogenized with a motorized Teflon/glass homogenizer (three times gentle stroke). The resulting homogenates containing both microsomal and cytosol fractions were suspended in 250 mM sucrose in 10 mM phosphate buffer, pH 7.4, and used within 24 h.

Preparation of Caco-2 Cell Lysate. After six mature (19−22 days postseeding) Caco-2 cell monolayers were washed twice with 3 mL of 37 °C HBSS (pH 7.4), they were cut out together with the porous polycarbonate membranes, immersed into 6 mL of 50 mM potassium phosphate buffer (pH 7.4), and sonicated in an ice bath (4 °C) for 30 min as described previously.[23,32]

Measurement of Protein Concentration. Protein concentrations of intestinal homogenates and cell lysates were determined using a protein assay kit (Bio-Rad, Hercules, CA), using bovine serum albumin as the standard.

Metabolism Studies Using Homogenates and Cell Lysate. Glucuronidation or sulfation of 10 μM formononetin by intestinal homogenates and Caco-2 cell lysate was measured using procedures described previously.[23,32] Slightly different solvent mixtures were used for the reactions where multidrug-resistance-related protein (MRP) (0.0625% ethanol and 0.0815% methanol in pH 7.4 10 mM KH_2PO_4) or OAT (0.1% dimethyl sulfone oxide and 0.4% methanol pH 7.4 10 mM KH_2PO_4) inhibitors were used due to the solubility of the inhibitors. Total content of organic solvents in all reactions was less than 0.5%, and was maintained at the same level for both control and actual experiments. Separate control experiments were performed for each solvent combination at the exact same concentration to minimize the potential biases that their use will introduce.

HPLC Analysis of Formononetin and Its Conjugates. The conditions for analyzing formononetin and its conjugates were the same as described before:[21,18] system, Agilent 1090 with diode array detector and ChemStation; column, Aqua (Phenomenex, Gilroy, CA), 5 μm, 150 × 4.5 mm; mobile phase A, 100% acetonitrile); mobile phase B, 0.04% (v/v) phosphoric acid plus 0.06% (v/v) triethylamine in water (pH 2.8); gradient, 0−3 min, 80% B, 3−23 min, 80−50% B, 23−25 min, 50% B, 25−26 min, 50−80% B, 26−28 min, 80% B; wavelength, 254 nm; and injection volume, 200 μL.

Data Analysis in the Caco-2 Cell Model. Rates of transport (B_t) were obtained using rate of change in concentration of transported formononetin or its metabolites as a function of time and volume of the sampling chamber (V) (eq 1).

$$B_t = \frac{dC}{dt}V \tag{1}$$

Apparent metabolic clearance (CL) of formononetin was calculated using rate of metabolite excretion (B_{ex}) divided by the initial concentration of formononetin at the loading side (C_i) (eq 2) as described previously.[32]

$$CL = \frac{B_{ex}}{C_i} \tag{2}$$

This is based on the assumption that the rate of excretion is related to initial concentration of formononetin.

(35) Hu, M.; Zheng, L.; Chen, J.; Liu, L.; Zhu, Y.; Dantzig, A. H.; Stratford, R. E., Jr. Mechanisms of transport of quinapril in Caco-2 cell monolayers: comparison with cephalexin. *Pharm. Res.* **1995**, *12*, 1120−1125.

(36) Liu, Y.; Liu, Y.; Dai, Y.; Xun, L.; Hu, M. Enteric Disposition and Recycling of Flavonoids and Ginkgo Flavonoids. *J. Altern. Complementary Med.* **2003**, *9*, 631−640.

Table 1. Effective Permeabilities or P^*_{eff} of Formononetin in the Two-Site Perfused Mouse or Four-Site Perfused Rat Intestinal Model[a]

	upper small intestine		lower small intestine	
mice	2.90 ± 0.69[b]		2.53 ± 0.17[c,d]	
	duodenum	jejunum	ileum	colon
rats[e]	2.38 ± 0.50	2.17 ± 0.34	1.06 ± 0.07	3.46 ± 0.30

[a] Data are presented as the mean ± SD of four determinations. [b] Not significantly different from rat duodenum ($p > 0.05$). [c] Not significantly different from rat jejunum ($p > 0.05$). [d] Significantly different from rat ileum ($p < 0.05$). [e] Reference 18.

Data Analysis in the Mouse Intestinal Perfusion Model. Dimensionless permeability of the formononetin was represented by P^*_{eff}, which was obtained as described previously.[18,34−36] Steady-state uptake of formononetin from the perfusate was measured by determining the rate of disappearance from the perfusate. Excretion rates of the metabolites were expressed as amounts of metabolites excreted per 30 min per 10 cm segment (nmol/30 min/10 cm).

Data Analysis in the Mouse Homogenate or Caco-2 Cell Lysate Model. Rates of metabolite formation in intestinal homogenate or Caco-2 cell lysate were expressed as amounts of metabolites formed per 30 min per 10 cm segment (nmol/30 min/10 cm) or each Caco-2 cell monolayer (pmol/min/monolayer) or per 4.2 cm^2. We normalize the rates to surface area or length of the intestine to facilitate the comparison between formation rates and excretion rates.

Statistical Analysis. Unpaired Student's *t* test (Microsoft Excel) was used to analyze the data. The prior level of significance was set at 5%, or $p < 0.05$.

Results

Regional Absorption and Metabolism of Formononetin in the Mouse Intestinal Perfusion Model. Absorption of formononetin (10 μM) in mouse intestine was rapid with minimal effects on water flux (i.e., water flux <0.5%/cm of perfused segment), regardless of whether inhibitors were used or not. This lack of effect on water flux is similar to results previously observed in the rat perfusion model.[17,18,29] There was no difference in the amounts of formononetin absorbed between two regions of the intestine. The amounts absorbed (36.0 nmol/30 min or 57% of perfused amount in ~10 cm upper small intestine; 30.5 nmol/30 min or 50% in ~10 cm lower small intestine) in mouse were similar to those in rats.[18] Dimensionless effective permeability of formononetin in the upper segment of mouse small intestine was similar to that in the rat duodenum, and that in the lower segment of mice was similar to that in rat jejunum but different from that in rat ileum ($p < 0.05$) (Table 1).

There were, however, significant differences in the excretion of phase II conjugates between rats and mice and between different segments of the mouse intestine. For example, formononetin sulfate was excreted in mice but not in rats.[18] A small amount of formononetin sulfate was also found in Caco-2 cells (see below). The amounts (nmol/30 min) of excreted glucuronide were slightly less than the amount of excreted sulfate in both segments, and more conjugates were excreted in the upper segment (9.79 ± 1.82 glucuronide vs 10.96 ± 0.72 sulfate) than in the lower segment (6.56 ± 1.03 glucuronide vs 7.99 ± 1.02 sulfate). On the other hand, the amounts of glucuronide excreted in mice were not significantly different from that in rats (Figure 1). Taken together, the total amounts of conjugates excreted in mice were significantly different from those in rats due to the excretion of sulfate in mouse intestine ($p < 0.05$) (Figure 1).

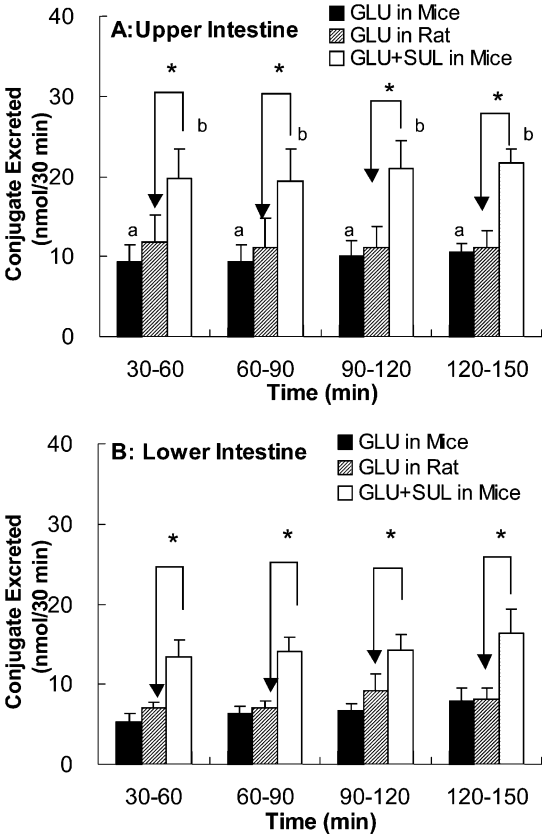

Figure 1. Amounts of conjugates excreted in (A) upper and (B) lower segments (10 cm) of intestine during two-site mouse intestinal perfusion (number of replicates (n) = 4). Perfusate containing 10 μM formononetin was used, and two segments of small intestine were perfused simultaneously at a flow rate of 0.191 mL/min. Amounts of conjugates excreted during 30 min perfusion, normalized to 10 cm intestinal length, were obtained as described in the Experimental Section. Each column represents the average of four determinations, and the error bar is the standard error (SE) of the mean. Solid, hatched, and blank columns represent amount of formononetin glucuronide (glucuronide) in mice and rats, and amount of glucuronide plus formononetin sulfate (sulfate) in mice during 30 min perfusion, respectively. Amounts of glucuronide in rat were from Jia et al.[18] There were statistically significant differences ($p < 0.05$) between amounts of conjugate excreted at different regions of the mouse intestine according to Student's *t* test (a and b). In the same region of the intestine, amounts of total conjugates excreted in mouse (glucuronide plus sulfate) were higher than amounts of those in rats ($p < 0.05$, arrows).

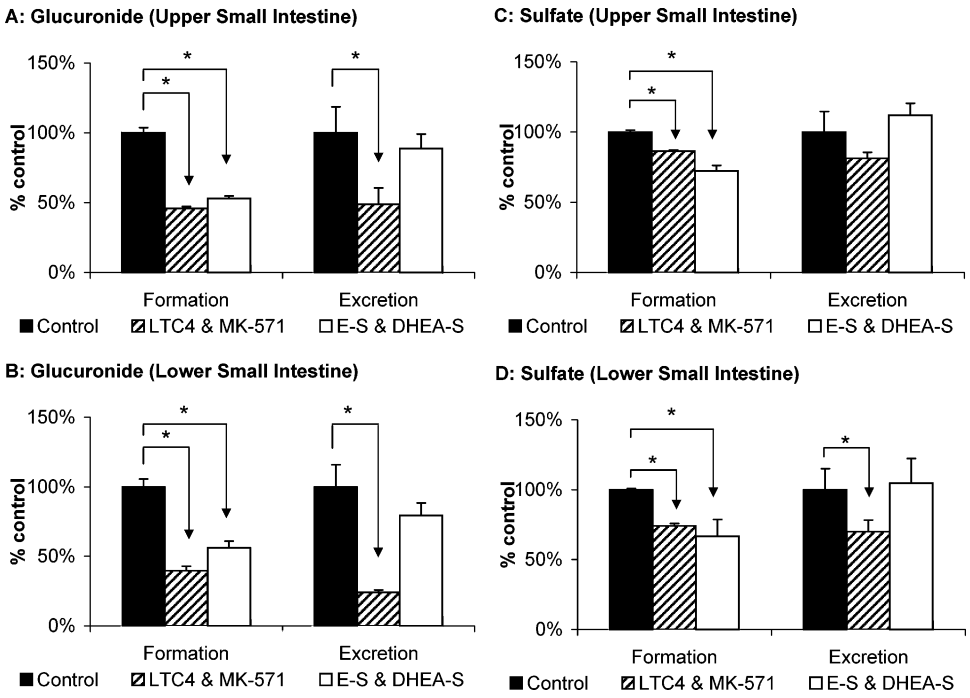

Figure 2. Effect of multidrug-resistance-related protein (MRP) and organic anion transporter (OAT) inhibitors on the formation and excretion of formononetin conjugates in the mouse small intestinal perfusion model. Rates of formation were determined from the reaction mixture containing formononetin (10 μM) with MRP inhibitors (0.1 μM leukotriene C_4, LTC_4, plus 50 μM MK-571) or OAT inhibitors (50 mM estrone sulfate, E-S, and 50 mM dihydroepiandrosterone sulfate, DHEA-S) in mouse intestine homogenates ($n = 3$). Rates of excretion were determined using perfusate containing formononetin (10 μM) with MRP inhibitors (0.1 μM LTC_4 plus 50 μM MK-571) or OAT inhibitors (50 mM E-S and 50 mM DHEA-S) in two-site mouse intestinal perfusion ($n = 4$), at a flow rate of 0.191 mL/min. Solid, hatched, and blank columns represent the control, MK-571 plus leukotriene C_4, and E-S plus DHEA-S treated group, respectively. Each data point represents the average of three (formation) or four (excretion) determinations, and the error bar represents the standard deviation (SD; for formation) or standard error (SE; for excretion) of the mean. The mean control values for formation rates ($\pm$SD or SE), which varied somewhat because of minor difference in the organic solvent used, are presented in Table 2. Controls containing different solvent mixtures were used due to the limit imposed by the solubility of different inhibitors as described in the Experimental Section. The asterisk (*) indicates a statistically significant difference ($p < 0.05$) compared to the control (i.e., formononetin only).

Table 2. Excretion and Formation Rates of Formononetin Metabolites in Mouse Intestine Models[a]

		glucuronide (nmol/min/10 cm)		sulfate (nmol/min/10 cm)	
small intestine	solvent	upper	lower	upper	lower
excretion rate		0.33 ± 0.06*[b]	0.22 ± 0.03*	0.36 ± 0.04*	0.27 ± 0.19*
formation rate	A[c]	7.13 ± 0.26	0.32 ± 0.02	0.87 ± 0.01	0.11 ± 0.001
	B[d]	10.04 ± 0.35	0.35 ± 0.02	1.08 ± 0.05	0.16 ± 0.01

[a] Excretion rates of the metabolites were expressed as amounts of metabolites excreted per min per 10 cm segment in the two-site intestinal perfusion model. Formation rates of the metabolites were obtained from the in vitro intestinal homogenate model using different solvent systems, and normalized to the length (10 cm) of intestine used to prepare the homogenate based on the protein concentration to compare with the excretion rates. Data are presented as the mean ± SD of four (excretion rates) or three (formation rates) determinations. [b] (*) $p < 0.01$ between excretion rate and formation rate. [c] Solvent A, used in experiments employing MRP inhibitors, is a mixture of 0.0625% ethanol and 0.0815% methanol in pH 7.4 10 mM KH_2PO_4. [d] Solvent B, used in experiments employing OAT inhibitors, is a mixture of 0.1% dimethyl sulfone oxide and 0.4% methanol in pH 7.4 10 mM KH_2PO_4.

To define the relative contribution of formation and the efflux step for the overall excretion of a certain metabolite, we compared the excretion rates during the intestinal perfusion with the formation rate obtained from in vitro metabolism experiments, both normalized to the length of the intestine used. We found that formation rates for glucuronide were 22−31 (in upper small intestine) and 1.5−1.6 (in lower small intestine) times faster than excretion rates (Table 2). The formation rate for sulfate was 2.4−3.0 times faster than excretion in the upper small intestine, but 60−40% slower than excretion in the lower small intestine (Table 2). We found that addition of an organic solvent mixture to the reaction media slightly increased the formation rates. This slight change (9%, 24%, 41%, 45%, or an average of 30%) may

Table 3. Rate of Formononetin Transport and Amounts of Its Excreted Metabolites in the Caco-2 Model[a]

	formononetin	GLU		SUL		
	rate of transport, nmol/h	AP side, nmol	BL side, nmol	AP side, nmol	BL side, nmol	total conjugates, nmol
control	4.21 ± 0.29	6.30 ± 1.21	3.73 ± 0.47	0.52 ± 0.07	0.17 ± 0.01	10.71
LTC4 and MK-571[b]	4.16 ± 0.17	0.37 ± 0.04[d]	0.44 ± 0.02[d]	0.26 ± 0.01[d]	0.23 ± 0.01[d]	1.29
E-S and DHEA-S[c]	4.10 ± 0.29	2.25 ± 0.37[d]	2.56 ± 0.36[d]	0.20 ± 0.03[d]	0.17 ± 0.02	5.19

[a] Rates of transport values were calculated using the first four data points (time = 0.5−2 h) in the amount transported versus time plot. Amounts of metabolites in the apical (AP) and basolateral (BL) media at the end of 7 h incubation were determined. Data are presented as the mean ± SD of three determinations. [b] Multidrug-resistance-related protein (MRP) inhibitors, LTC_4 (0.1 μM) plus MK-571 (50 μM), were added simultaneously into the AP side with formononetin (10 μM). [c] Organic anion transporter (OAT) inhibitors (50 mM estrone sulfate plus 50 mM DHEA sulfate) were added simultaneously into the AP side with formononetin (10 μM). [d] $p < 0.05$ between control and treated group.

Table 4. Excretion and Formation Rates of Formononetin Metabolites in Caco-2 Models[a]

	solvent	glucuronide (pmol/min/monolayer)	sulfate (pmol/min/monolayer)
excretion rate		16.7347 ± 3.8032*[b]	1.8409 ± 0.1679*
formation rate	A[c]	0.8286 ± 0.0524	0.0709 ± 0.0041
	B[d]	2.5931 ± 0.0440	0.2174 ± 0.0793

[a] Excretion rates of the metabolites were expressed as total amounts of metabolites excreted into both apical and basolateral sides per min per monolayer in the Caco-2 transport model. Formation rates of the metabolites were obtained from the in vitro Caco-2 cell lysate model using different solvent systems, and normalized to one monolayer used to prepare the cell lysate based on the protein concentration to compare with the excretion rates. Data are presented as the mean ± SD of three determinations. [b] (*) $p < 0.01$ between excretion rate and formation rate. [c] Solvent A, used in experiments employing MRP inhibitors, is a mixture of 0.0625% ethanol and 0.0815% methanol in pH 7.4 10 mM KH_2PO_4. [d] Solvent B, used in experiments employing OAT inhibitors, is a mixture of 0.1% dimethyl sulfone oxide and 0.4% methanol in pH 7.4 10 mM KH_2PO_4.

be the result of solvent effects. As a consequence, we always run multiple control experiments, each for a solvent combination in order to sort out the effects of these solvent mixtures.

In contrast to intestinal perfusate, sulfate was not detected although glucuronide was detected in mouse bile.[18] However, the amount of glucuronide excreted in mouse bile was approximately 120-fold lower than in rat bile (0.81 vs 96 nmol/120 min per 2-site perfusion or 0.18% and 20.94% dose/120 min per 2-site perfusion), primarily because the amount of bile produced was about 200 times smaller.

Effect of MRP or OAT Inhibitors on Absorption and Metabolism of Formononetin in the Mouse Perfusion Model. Formation and excretion rates in the absence or presence of anion transporter inhibitors were determined to delineate the possible involvement of transporters on the disposition of formononetin conjugates. Two multidrug-resistance-related protein (MRP) inhibitors, leukotriene C_4 (LTC_4, 0.1 μM) plus MK-571 (50 μM), were used together. In the mouse perfusion model, they significantly decreased the excretion of glucuronide in both upper (51%) and lower (76%) small intestine (Figure 2A,B) and the excretion of sulfate in lower mouse small intestine (30%) (Figure 2D). They also significantly decreased the formation rates of both conjugates in homogenates prepared from the upper (54% for glucuronide, 13% for sulfate; Figure 2A,C) and the lower (60% for glucuronide, 26% for sulfate; Figure 2B,D) small intestine.

On the contrary, organic anion transporter (OAT) inhibitors (50 mM estrone sulfate plus 50 mM dihydroepiandrosterone [DHEA] sulfate) did not significantly change the excretion of formononetin conjugates in either the upper or the lower small intestine (Figure 2). However, they significantly decreased the formation rates of both conjugates in intestinal homogenate prepared from upper (47% for glucuronide, 27% for sulfate; Figure 2A,C) and lower (44% for glucuronide, 33% for sulfate; Figure 2B,D) small intestine.

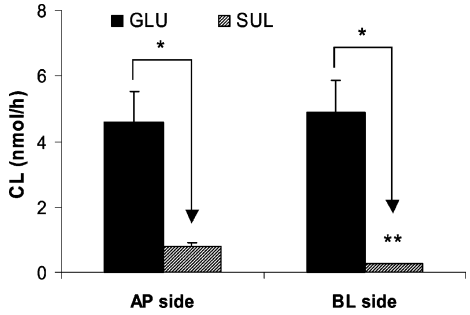

Figure 3. Excretion of formononetin metabolites in the Caco-2 model. Formononetin (10 μM) was added to the apical (AP) side of the Caco-2 cell monolayer, and the clearance (CL) of formononetin glucuronide (glucuronide; solid columns) and formononetin sulfate (sulfate; hatched columns) on the AP and basolateral (BL) sides of the monolayers was determined as described in the Experimental Section. Each column represents the mean of three determinations, and the error bars are standard deviations of the mean. The asterisk (*) indicates a statistically significant difference ($p < 0.05$) between glucuronide and sulfate, and the pair of asterisks (**) indicates a statistically significant difference ($p < 0.05$) between apical and basolateral excretion.

Absorption and Metabolism of Formononetin in the Caco-2 Model. Significant amounts of formononetin (10 μM at the donor side) were metabolized into glucuronide and sulfate (total 11 nmol/monolayer at 7 h) during its transport

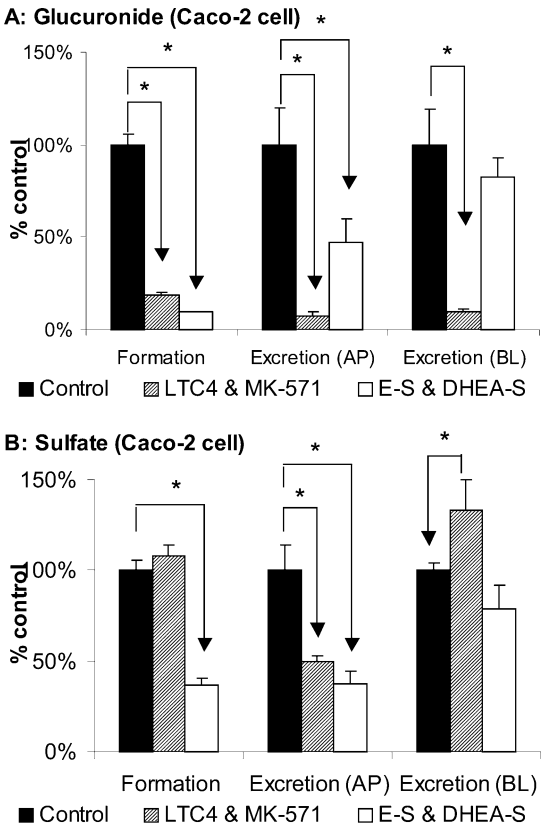

Figure 4. Effect of multidrug-resistance-related protein (MRP) and organic anion transporter (OAT) inhibitors on the formation and excretion of formononetin conjugates in the Caco-2 model. Rates of formation were determined from the reaction mixture containing formononetin (10 μM) with MRP inhibitors (0.1 μM leukotriene C_4, LTC_4, plus 50 μM MK-571) or OAT inhibitors (50 mM estrone sulfate, E-S, and 50 mM dihydroepiandrosterone sulfate, DHEA-S) in Caco-2 cell lysate (n = 3). Rates of excretion of the conjugates into the apical (AP) and basolateral (BL) sides were determined using solution containing formononetin (10 μM) with MRP inhibitors (0.1 μM LTC_4 plus 50 μM MK-571) or OAT inhibitors (50 mM E-S and 50 mM DHEA-S) in the Caco-2 cell culture model (n = 3). Solid, hatched, and blank columns represent the control, MK-571 plus leukotriene C_4, and E-S plus DHEA-S treated group, respectively. Each data point represents the average of three determinations, and the error bar represents the standard deviation (SD) of the mean. The mean control values for formation rates (±SD or SE), which varied somewhat because of minor difference in the organic solvent used, are presented in Table 4. The asterisk (*) indicates a statistically significant difference ($p < 0.05$) compared to the control (i.e., formononetin only).

across the Caco-2 cell monolayers (Table 3). More glucuronide was excreted than sulfate, and amounts excreted were polarized with larger amounts of both found at the apical side (Table 3), which is similar to our previously reported result.[18] Metabolic clearances (CL) for glucuronide were higher (12-fold in the AP side, 19-fold in the BL side) than those for sulfate in the Caco-2 cell monolayer (Figure 3). CLs for glucuronide in both sides of the cell monolayers were not different from each other. However, CL for sulfate was higher in the AP side than in the BL side ($p < 0.05$) (Figure 3). Excretion rates (B_{ex}) of both conjugates from the Caco-2 cell monolayer were significantly higher (6−20 and 8−26 times for glucuronide and sulfate, respectively) than the formation rates in the cell lysate (B_{met}) (Table 4).

Effect of MRP or OAT Inhibitors on Absorption and Metabolism of Formononetin in the Caco-2 Model. Formation and excretion rates in the absence or presence of anion transporter inhibitors were obtained to determine the possible involvement of transporters on the disposition of formononetin conjugates in the Caco-2 cell culture model. Multidrug-resistance-related protein (MRP) inhibitors, LTC_4 (0.1 μM) plus MK-571 (50 μM), significantly decreased the excretion rate of glucuronide into both sides (93% for the AP side, 90% for the BL side) and sulfate into the AP side (50%), but increased the BL excretion rate of sulfate (33%). They also decreased the formation rate of glucuronide (81%) but did not change the formation rate of sulfate (Figure 4).

On the contrary, organic anion transporter (OAT) inhibitors (50 mM estrone sulfate plus 50 mM DHEA sulfate) significantly decreased the formation rate of both glucuronide (90%) and sulfate (64%) in Caco-2 cell lysate. They also decreased the AP excretion rates of both glucuronide (63%) and sulfate (62%) but did not change the BL excretion rates of either conjugate (Figure 4).

Discussion

One of the main reasons why flavonoids have poor bioavailability is because they participate in metabolic recycling processes including both enteric and enterohepatic recycling.[16,17] Enteric recycling is enabled by enteric excretion of phase II conjugates whereas enterohepatic recycling is enabled by the hepatic excretion of phase II conjugates. Both recycling processes need the involvement of microbial hydrolysis of flavonoid conjugates to regenerate aglycons so they can be recycled into the systemic circulation following their colonic reabsorption. Recently, we proposed that the enterohepatic and enteric recycling are enabled by the coupling of efflux transporters and conjugating enzymes (or "enzyme-transporter coupling") in intestine and liver.[37]

Previously, we have used the rat intestinal perfusion model to determine mechanisms responsible for intestinal disposition of flavonoids via enteric recycling. However, we found very little or no sulfated flavonoid conjugates in the rat intestinal perfusate.[16−18] Since sulfated conjugates represent important metabolites in humans, we thought that an alternative animal model would be useful. Furthermore, genetically manipulated rats are rare, which makes it difficult to determine the role of a particular efflux transporter or conjugating enzyme in vivo. The latter is needed to determine how the coupling of efflux transporter and conjugating

(37) Jeong, E. J.; Liu, X.; Jia, X.; Chen, J.; Hu, M. Coupling of Conjugating Enzymes and Efflux Transporters: Impact on Bioavailability and Drug Interactions. Unpublished results.

enzymes affect bioavailabilities of flavonoids and other xenobiotics.

In the present study, we conducted studies to determine if the mouse intestinal perfusion model can be used for studying conjugation of flavonoids. We have chosen formononetin as our model compound since it has only one phenolic group and therefore is ideally suited to determine the relative contribution of both conjugation pathways. Previously, we only detected glucuronidated formononetin in rat intestinal perfusate.[18]

The results showed that the mouse intestinal perfusion model may be better suited than the rat model in determining the intestinal disposition of flavonoids for the following reasons. First, perfusion had minimal effects on water flux (i.e., water flux < 0.5%/cm of perfused segment), which is similar to what we observed in the rat perfusion model. This suggests that mouse intestinal viability is well maintained, based on our prior experience with the rat intestine in that deterioration of the intestinal epithelium is often associated with a large increase in water flux.

Second, the absorption and the dimensionless permeabilities of formononetin in mouse small intestine were similar to that in rat small intestine (Table 1). The slightly higher amounts absorbed in mouse were not statistically significantly different from those in rats (Table 1). In spite of the relatively short length of mouse small intestine (about 25−30 cm) compared to rats (about 80−100 cm), permeabilities in the upper and lower segments of mouse intestine correspond to those in the duodenum and jejunum of rats (Table 1). It suggests that mouse small intestine is not significantly different form rat small intestine in terms of formononetin permeability.

Third, metabolite excretion was also site-dependent in mouse intestine as in the rat intestine. More metabolites (33−75% for glucuronide, 28−44% for sulfate, $p < 0.05$) were excreted in upper than lower small intestine, just as reported for the rat intestine.[18] Additionally, when comparing excretion of glucuronidated formononetin into intestinal lumen, the amounts excreted in mouse intestine were not significantly different from those in rat intestine.

Aside from the above demonstrated similarities, certain distinctive characteristics in the mouse intestinal perfusion model demonstrated that it may be better than the rat model. Specifically, the mouse model showed a pattern of metabolite excretion different from that of the rat model. For example, sulfated formononetin, which was barely detected in the rat model, was detected in mouse intestinal perfusate at amounts comparable to that of glucuronide (Figure 1).

To further demonstrate the utility of the mouse model, we then determined which step, formation or transport, is the rate-determining step for the intestinal excretion of phase II conjugates of formononetin using the mouse model. Compared to the Caco-2 model, in which formation served as the rate-limiting step for both glucuronide and sulfate (Table 4), mouse intestinal excretion of glucuronides was rate-limited by efflux transporter in upper and lower intestine (Table 2). On the other hand, mouse intestinal excretion of sulfate was rate-limited by the efflux transporter only in upper intestine but not in lower intestine (Table 2). The results are not different from those shown for rat intestine where excretion of formononetin glucuronide is also rate-limited by efflux transporters.[18] The latter is based on estimation that 10 cm of small intestine will yield about 3 mg of microsomal proteins, which translates to a total conjugation rate of more than 80 nmol/30 min/10 cm, much faster than the excretion rate of no more than 20 nmol/30 min/10 cm.

Last, we determined which transporter(s) is (are) involved in the excretion of the conjugates using efflux transporter inhibitors, which we had not done in rat perfusion studies. The transporter inhibitors, MRP and OAT inhibitors, were chosen on the basis of the previous finding that MRP and OAT are involved in the intestinal efflux of these hydrophilic phase II conjugates of flavonoids and drugs in the Caco-2 cell culture model.[14,17,21,32] We found that in the mouse perfusion model excretion of glucuronide was inhibited by 58% (upper segment) to 74% (lower segment) in the presence of MRP inhibitors but not affected by OAT inhibitors, whereas the excretion of sulfate was not substantially inhibited by either MRP or OAT inhibitors even though a moderate inhibition of sulfate excretion by 25% ($p < 0.05$) was observed in the presence of MRP inhibitors. The results in mice were confirmed by Caco-2 results in that the main pathway for glucuronide in the Caco-2 model appears to be MRP since use of two MRP inhibitors inhibited both AP and BL excretion by more than 90% (Figure 4). It is also consistent with the presence of MRP2 in the upper and lower intestine of the mouse.[38] The main pathway for sulfate in the Caco-2 cells is less well-defined since its excretion was inhibited by no more than 55% by selected MRP or OAT inhibitors. Contributions from apical MRP and OAT are likely, and additional contributions from other transporter-(s) are possible for sulfate excretion. One such transporter is BCRP1 as recently described by Adachi et al.[39]

The inhibition of conjugate formation by OAT inhibitors probably did not materialize inside cells on the basis of the following findings. Inhibition of conjugate formation (both glucuronide and sulfate) by OAT inhibitors did not translate into inhibition of excretion, since the extent of excretion inhibition was less than the formation inhibition (at best, the same as formation inhibition for AP sulfate excretion) probably due to poor access of OAT inhibitors to the intracellular domain owing to the hydrophilic nature of the hormone sulfates (e.g., estrone sulfate and DHEA sulfate). On the other hand, it is more difficult to judge if effects of MRP inhibitors on cellular excretion of metabolites were due

(38) Stephens, R. H.; O'Neill C. A.; Bennett, J.; Humphrey, M.; Henry, B.; Rowland, M.; Warhurst, G. Resolution of P-glycoprotein and non-P-glycoprotein effects on drug permeability using intestinal tissues from mdr1a (-/-) mice. *Br. J. Pharmacol.* **2002**, *135*, 2038−2046.

(39) Adachi, Y.; Suzuki, H.; Schinkel, A. H.; Sugiyama, Y. Role of breast cancer resistance protein (Bcrp1/Abcg2) in the extrusion of glucuronide and sulfate conjugates from enterocytes to intestinal lumen. *Mol. Pharmacol.* **2005**, *67*, 923−928.

to metabolism or excretion or both. This is because the excretion is severely affected, and much more than expected from the inhibition of transporters or enzyme alone. We believe that both may be affected since MK-571 can gain limited access to the cellular domain (e.g., permeability of MK-571 in the Caco-2 cell model was 6.1×10^{-6} cm/s at 10 μM and 9.2×10^{-6} cm/s at 50 μM; unpublished data), although the concentration inside the cells must be much lower than those at the outside.

In conclusion, this is the first report that the mouse intestinal perfusion model is superior in understanding the disposition of flavonoids since mouse intestine metabolized formononetin into sulfated conjugates, as expected from human intestine. In addition, the excretion of conjugates appeared to be mediated by efflux transporters, allowing the mouse model to be used to investigate the coupling of sulfotransferase and organic anion transporters such as MRPs. Because of the availability of genetically modified mouse, this technique may be especially suited for understanding the coupling of the conjugating enzymes and efflux transporters responsible for removing hydrophilic conjugated metabolites from the intestine.

Acknowledgment. We thank Huimin Lin, College of Pharmacy, Washington State University, for her technical contribution to the mouse surgery and cell culture. This study was supported by National Institutes of Health (NIH) Grant CA 87779.

MP0498852